IEEE Access
Multidisciplinary | Rapid Review | Open Access Journal

Received 25 March 2024, accepted 27 April 2024, date of publication 8 May 2024, date of current version 15 May 2024.

Digital Object Identifier 10.1109/ACCESS.2024.3398411

METHODS

Biosensing of Circulating Tumor Cells With a Microcavity Embedded With Pico-Porous Nanostructured Chips

SHENG-WEN CHEN[1], JANNE-WHA WU[1], (Member, IEEE), AND CHUNG-ER HUANG[2]
[1]Department of Electrical Engineering, National Chung Cheng University, Chiayi City 621301, Taiwan
[2]Cytoaurora Biotechnologies Inc., Hsinchu Science Park, Hsinchu 30261, Taiwan

Corresponding author: Janne-Wha Wu (jwwu@ccu.edu.tw)

This work was supported in part by the National Science and Technology Council, Taiwan, under Grant MOST111-2221-E-194-011- and Grant MOST111-2218-E-194-004-; and in part by the Ministry of Education, Taiwan.

ABSTRACT Circulating rare cells (CRCs) in the peripheral blood are considered crucial cells in pathological phenomena. Circulating tumor cells (CTCs) detach from solid tumors via blood transport and play a crucial role in cancer metastasis, which is the primary focus of CRCs research. Therefore, a simple and cost-effective device for capturing and culturing CTCs is required for pathological analysis. This study proposes a new biosensing device that includes a pair of surface-modified pico-porous nanostructured chips with a large cross-section and contact area. Compared to traditional narrow microfluidics, this study features a lower shear stress force, resulting in less damage to the captured cells (less than 5%). In addition, unlike devices with non-nanostructured silicon chips, this microcavity biosensing device can provide approximately ten times the cell capture rate and maintain the captured cells as living cells. Another important point to note is that captured live cells can be cultured for up to 18 days or longer. Computer-aided cell image recognition was utilized to minimize human misjudgment and to reduce the analysis time to less than 30 minutes. The novelty of this research is the improved capture rate of CTCs and the prolonged survival time of cells in culture achieved through the utilization of the newly proposed device.

INDEX TERMS Circulating rare cells, circulating tumor cells, microfluidics, microcavity biosensing, shear stress force, pico-porous nanostructured chip.

I. INTRODUCTION

Circulating rare cells (CRCs), regarded as rare nucleated cells in the peripheral blood, are associated with certain diseases or the physiological characteristics of subjects. Therefore, they are widely used in auxiliary non-invasive diagnostic inspections. Cell types include circulating tumor cells (CTCs) [1], megakaryocytes [2], fibroblast-like cells [3], and nucleated red blood cells [4]. Cancer is one of the top ten causes of death worldwide. Although they have a significant impact on human health, diagnostic methods are complex and costly. CTCs can provide comprehensive biological information about cancer cells. Therefore, how to increase the effective capture of CTCs from the peripheral blood is worthy of study.

At present, cell size [5], [6], magnetic materials [7], [8], [9], and microfluidics [10], [11], [12] are the three most commonly used methods for cell capture and counting. In addition to these techniques, there are also some studies of using dielectrophoresis (DEP) [13], [14], circuit-based [15], and microwave [16], [17]. Some studies have combined various techniques to enhance capture rates [18], [19], and cell culture monitoring [20]. Some considerations are considered in the choice of capture technologies, such as the requirement of specific equipment and the potential impact on cells. For example, screening cells based on size always results in missing the capture of smaller cells [21], and the internalization of magnetic force affects the proliferation and metabolism of captured cells [22]. Microfluidic technology also faces challenges, such as the shear stress force that can easily damage cells [23] and the cell capture rate being affected by laminar flow [24].

The associate editor coordinating the review of this manuscript and approving it for publication was Wu-Shiung Feng.

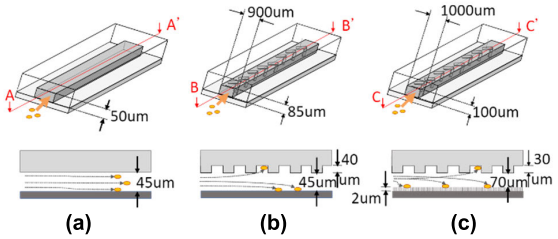

FIGURE 1. (a) Flat-walled microfluidic [24]; (b) Herringbone microfluidic with glass substrate [25]; (c) Herringbone microfluidic with nanostructured substrate [26].

To solve the problems encountered in microfluidic channels, some researchers have utilized a herringbone structure, as shown in Fig. 1(b), to induce turbulence and solve the laminar flow problem [25]. However, this approach also increases the risk of target cells adhering to the herringbone structure, thereby reducing the capture rate of target cells in the microfluidic capture area [26]. In addition, some researchers have utilized nanostructures, as shown in Fig. 1(c), to enhance the capture rate of target cells [27], [28]. However, this approach may increase the risk of shear stress force on cells, which can result in cell damage [29], [30], and deformation [31], [32]. However, there is a lack of research on the utilization of nanostructures to successfully capture and culture cells. In a paper published in 2007, W. Kim [33] used nanowires to capture cells and cultured them for three days to demonstrate the feasibility of using this structure for cell capture and culture. This information was used as an important reference in this study. In addition, reducing the damage caused by cells during capture and the successful culturing of captured living cells is a significant challenge. When pushing the liquid specimen through the microfluidic path, the shear stress force generated by thrust is almost unavoidable. Shaking is another factor that generates a shear stress force that prevents cell stacking by reducing the cell capture rate. Hence, the focus of this study was to reduce the various shear stress forces generated during the cell capture process and create a microenvironment that facilitates the extension of filopodia. The main features of this study are as follows:

1.Pico-porous nanostructures for enhancing the capture rate of target cells.

2.Microcavity for high cell survival and cell culture success rate due to low shear stress force.

3.Use a low shaking speed to minimize cell stacking.

II. BIOSENSING FIXTURE

The microcavity biosensing fixture comprised a bottom carrier (A1), top carrier (A2), and guide frame (N1), which were fabricated using polylactic acid (PLA) as the raw material using a 3D printer (INFINITY3DP X1E-Plus). Two nanostructured silicon chips (C1 and C2) with a pico-porous morphology were fabricated using Metal-Assisted Chemical Etching (MACE). Fig. 2 shows the exploded view in (a), the assembly drawing in (b), and the photograph in (c).

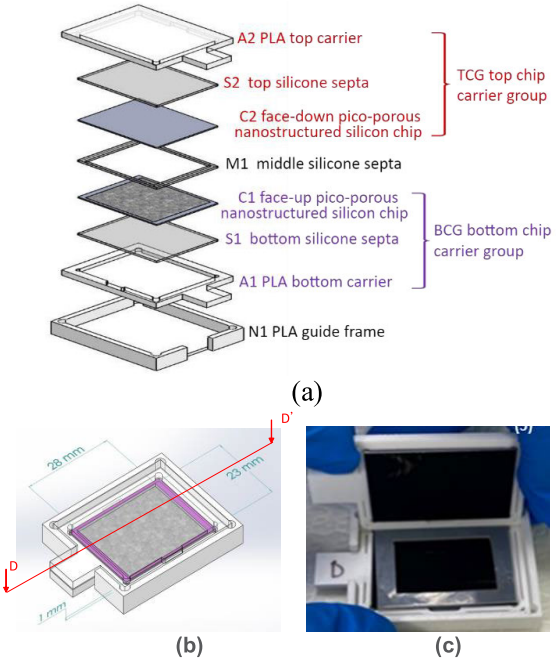

FIGURE 2. (a) An exploded view of a microcavity biosensing fixture with nanostructured silicon chips; (b) Complete assembly of the fixture jig identified with dimension; (c) Fixture photo.

The microcavity biosensing assembly process was conducted as follows:

1.First, 10 μL of DI water was dropped onto the PLA bottom carrier (A1) and PLA top carrier (A2) (the internal dimensions of A1 and A2 were fitted with the chip size).

2.Insert the 1 mm bottom silicon septa (S1) above the bottom carrier (A1) and then place the top silicon septa (S2) under the top carrier (A2). DI water was used to bond the carriers and the silicon septa together.

3.The middle silicone septa (M1) was surrounded by a face-up pico-porous nanostructured chip (C1) and a face-down pico-porous nanostructured chip (C2). M1 builds the reaction area on the face-up pico-porous nanostructured chip (C1) and prevents the liquid specimen from overflowing.

4.Next, 200 μL of the liquid specimen was injected with H1975 cells into the center of the face-up chip (C1). Subsequently, the top chip carrier group (TCG) and the bottom chip carrier group (BCG) were stacked and clamped using a PLA guide frame (N1) fixed with two dovetail clips.

5.Finally, ensure that they are sealed to create a microcavity for capturing cells.

The nanostructured silicon chip was manufactured using a single-sided polished boron-doped p-type (100) silicon wafer with a thickness of 650 μm and resistivity of 0.001–0.005Ω·cm. Before proceeding with the fabrication step, the wafers were immediately removed from environmental contaminants and organic residues, following standard RCA cleaning. In the first step, silver ions were deposited on the wafers in a mixed solution of hydrofluoric acid (HF) and silver nitrate ($AgNO_3$) for 60 s. Wafers were etched using a mixed solution of HF and H_2O_2 for 30 min at room

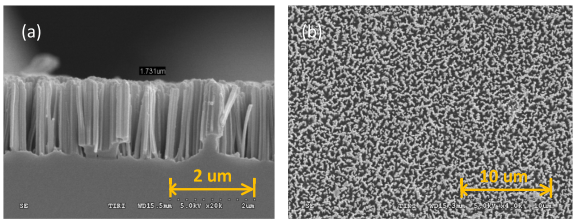

FIGURE 3. Pico-porous nanostructured chip SEM (a) Cross-section; (b) Top view.

temperature in the dark. The wafers were then placed in a mixed solution of CH_3OH, HNO_3, and H_2O_2 for 45 min to remove silver ions. To prevent contamination of the chip, the wafers were initially cut into chips with a laser after fabrication of the porous nanostructure. The chips were subjected to surface treatment by silane deposition and streptavidin covalent binding. This step was crucial for cell capture. The chips with pico-porous structures will increase the contact area between the pseudopodia of CTCs and the chip, enabling the pseudopods to firmly grasp, leading CTCs to believe they can move and metastasize. Fig. 3(a) shows the cross-section of a completed pico-porous nanostructured chip, the 1.731 $\boldsymbol{\mu m}$ long columnar structure in the picture has pico-sized holes on its top surface. Fig. 3(b) shows the top view.

The fixture was shaken using an orbital shaker (Major Science, NOR-30) as shown in Fig. 4(a). The shaking process consisted of two cycles: 30 minutes initially at 20 rpm, followed by a slow rotation of 180° to the other side for another 30 minutes at 20 rpm. Fig. 4 (b) and (c) show the cross-sectional views of these two cycles. Two pico-porous nanostructured chips can effectively capture target cells during shaking. The use of low-speed rotational shaking during the capture process can reduce the cell accumulation and enhance the cell capture rate.

After the cell capture process was completed, the two nanostructured chips were separated and rinsed with Dulbecco's phosphate-buffered saline (DPBS) to ensure that only the target cells remained on the chip. The chips were photographed using a fluorescence microscope for analysis, and the captured target cells were counted.

III. SHEAR STRESS FORCE DURING CELL CAPTURE

Different methods used to enhance the cell capture rate result in varying shear stress forces. Two of the most important types of shear stress force damage may occur during the process of injecting the liquid specimen into the microcavity fixture, and rotating and shaking the jig. This is discussed in the following two sections:

A. SHEAR STRESS FORCE IN THE LIQUID SPECIMEN INJECTION PROCESS

In current research, the fluid shear stress force in the flow channel used for cell capture is mostly discussed based on Hagen–Poiseuille's equation.

The shear stress force (τ) is defined by the volumetric flow rate (Q), viscosity of the media (μ), and dimensions of the microfluidic features (such as the width (w) and height (h) of a rectangular channel or the radius (R) of a circular channel). The shear stress force depends on the shape of the structure, and can be approximated using Poiseuille's equation [34].

TABLE 1. Comparison of calculated shear stress data.

Pipe shape	Width(w) mm	Height(h) mm	Radius(R) cm	Flow Rate (Q)	Shear stress dyn/cm^2
Rectangular [This study]	23	1	NA	~100 $\mu L/h$	4.46×10^{-3}
Rectangular [37]	1	0.1	NA	100 $\mu L/h$	10.26
Circular [36]	NA	NA	7.94×10^{-3}	20 $\mu L/s$	510

The average velocity of the flow $\bar{u}$ is

$$\bar{u} = \frac{Q}{\pi R^2} \tag{1}$$

For Poiseuille flow shear stress force

$$(\tau_{cir}) = \frac{4\mu\bar{u}}{R} \tag{2}$$

By substituting (1) into (2), we can obtain the shear stress force in a circular pipe.

$$(\tau_{cir}) = \frac{4 \times \mu \times Q}{\pi R^3} \tag{3}$$

In 1998, Bhat [35] described the shear stress force in a rectangular pipe using the following equation.

$$(\tau_{rect}) = \frac{6 \times \mu \times Q}{wh^2} \tag{4}$$

From (3) and (4), the relationship between the size of the cross-sectional area and shear stress force in the microfluidic structure has the greatest impact. The larger the cross-sectional area, the smaller is the shear stress force.

To minimize the impact of the shear stress force on the cell-capturing process of biosensing, a microcavity was utilized in this study, as shown in Fig. 2. Compared to traditional narrow microfluidics, this microcavity structure is 23 times wider and 10 times higher than previously published results [37]. In this study, the flow rate was 100 $\mu L/h$ as in the case of [37], but the shear stress force was only 0.00446 dyn/cm^2 owing to the large cross-section, which is 1/2300 times that of [37]. Table 1 summarizes the results of this study and other published results. It can be seen from the table that compared to the other cell capture structures. The shear stress force of the microcavity structure was relatively low.

B. SHEAR STRESS FORCE OCCURS DURING ROTATIONAL SHAKING

It is equipped with shaking equipment commonly used in biological experiments such as solution mixing and cell culture [38]. Klaus. In 1989, Ley [39] proposed the use of shaking to apply shear stress and test its impact on cells. He proposed the following mean shear-stress force:

$$\bar{\tau} = \frac{\sum(\tau(r) \cdot \mathrm{A}(r))}{\sum \mathrm{A}(r)} \tag{5}$$

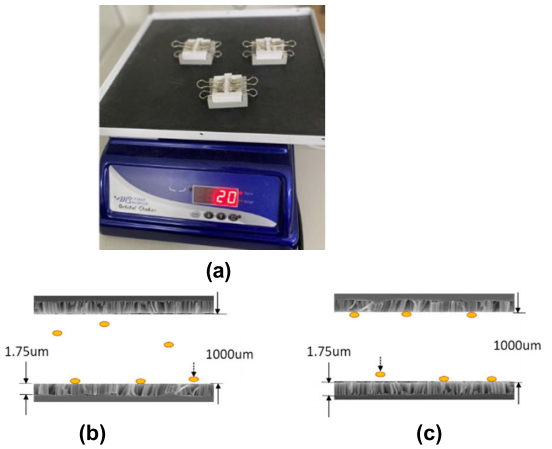

FIGURE 4. (a) Samples on shaking equipment; (b) Illustrations of pico-porous nanostructured chips capturing the target cells over the D-D' section of Fig. 2(b) During the first 30 minutes shaking cycle; (c) Another 30 minutes shaking cycle conducted after turning the jig upside down.

TABLE 2. Comparison of calculated shaking shear stress data.

	Radius (a)cm	Viscosity (η) poise	Density (ρ) g/ml	Frequency (f) rotations/s	Shear stress (τ_{max})dyn/cm^2
This study	1	1	0.0075	20/60	0.26
[39]	0.43	1	0.0075	50/60	0.44
	0.43	1	0.0075	100/60	1.25
	0.43	1	0.0075	150/60	2.29
[40]	1.4	1	0.0075	25/60	0.5
	1.4	1	0.0075	100/60	4.1
	1.4	1	0.0075	200/60	11.5

where $\tau(r) = \gamma(r) \cdot \eta$ and $\gamma\,(r) = \frac{2\pi\tau f}{hc}$ are calculated from the actual geometry of the plate-and-cone instrument using area weighting (A). The (r) is radius of plate-and-cone, (h) is slit height and (f) is rotation frequency.

The maximal wall shear stress force at the bottom of the dish can be simplified as

$$(\tau_{shaking\_max}) = a\sqrt{\eta\rho(2\pi f)^3} \tag{6}$$

where (a) is the radius of orbital rotation, (ρ) is the density of the culture medium, (η) is the viscosity of the medium, and (f) is the frequency of rotation and the maximal shear stress $\tau_{shaking\_max}$.

Higher shear stress forces resulting from high rotational shaking speeds can adversely affect target cells. As referenced [40], the rotational shaking speed during the biosensing capture process must be less than 100 rpm. Some studies have utilized an orbital shaker to simulate cells in the blood flow [41]. The shear stress forces applied in these studies were relatively high. Therefore, shaking speed should not be too high to prevent cell stacking. In this study, the purpose of using low-speed rotation at 20 rpm with an orbital shaker was used to reduce laminar flow and cell accumulation. The study indicates a low shear stress force of 0.26 dyn/cm^2 which is 1/10 times that at 150 rpm [39]. It also effectively enhanced the capture rate of the target cells. Even if the target cells are not captured by the face-up chip owing to accumulation, they can be captured by the face-down chip after rotating the microcavity 180°. This method demonstrated the high

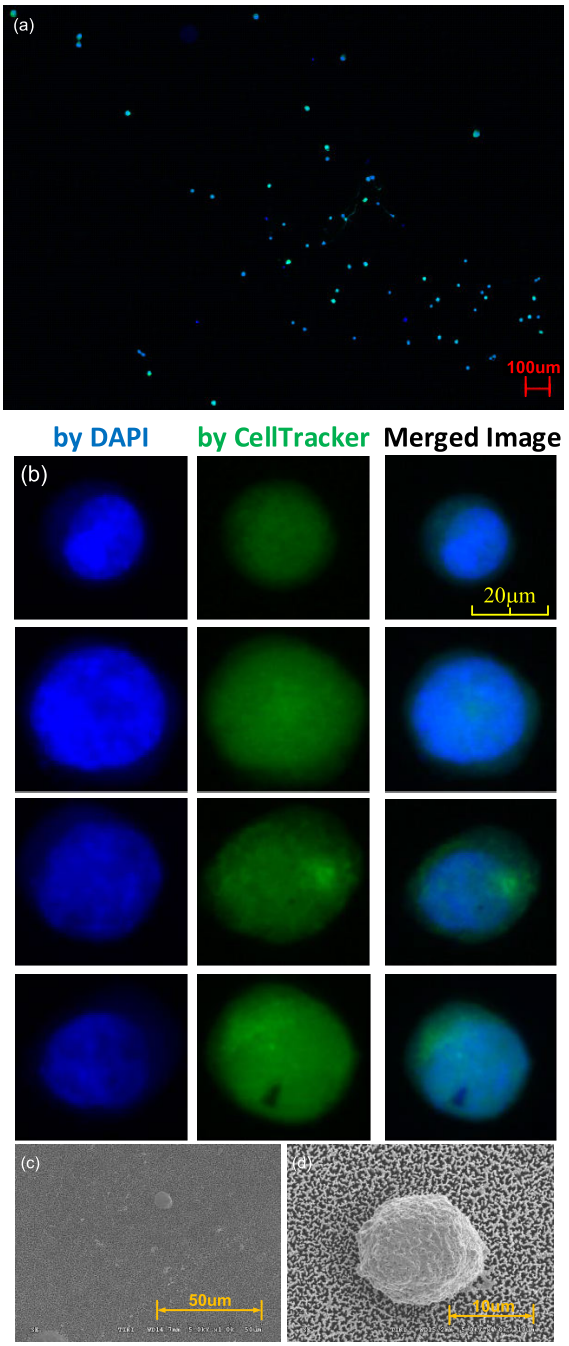

FIGURE 5. (a)Diagram of the distribution of cells on the chip; (b) Several computer-aided fluorescent-dyeing stain images of H1975 cells in Fig 4(a); (c) H1975-cells top view; (d) H1975 cells close-up photo.

efficiency of a simple capture process. Table 2 provides a summary comparing the findings of this study with those of other published studies. It can be seen from the table that compared to other rotation speeds, the shear stress force of the microcavity structure is relatively low.

IV. MATERIAL AND METHODS

A. PREPARATION OF CIRCULATING TUMOR CELL LINES

The lung cancer cell line H1975 (Human lung cancer cells, ATCC CRL-5908^{TM}, Manassas, VA, USA) were maintained

in an incubator at 37°C and 5% CO_2 in RPMI-1640 medium (Gibco, Grand Island, NY, USA) supplemented with 10% fetal bovine serum (FBS) and 100 *units/mL* antibiotic-antimycotic (Gibco, Grand Island, NY, USA).

During the initial stage of the cell capture experiment, CellTracker™Green CMFDA Dye (Thermo Fisher Scientific, Eugene, OR, USA) was added to the H1975 cell medium and incubated at 37°C for 30 minutes. Subsequently, H1975 cells were fixed with 4% paraformaldehyde (PFA) for 15 minutes. The fixed cells were incubated with biotinylated anti-EpCAM and anti-E-cadherin capture antibodies at 37°C. After 30 minutes, the samples were centrifuged at 300 × g for 10 minutes to collect cell pellets. All cell pellets were resuspended in 200 μL DPBS, and 4',6-diamidino-2-phenylindole (DAPI) was added to stain the nuclei, which served as a model for evaluating capture efficiency.

Biotinylated anti-EpCAM and E-cadherin capture antibodies were added to the H1975 cell medium and incubated at 37°C for 30 minutes. H1975 cells were used in a live cell culture experiment and then centrifuged at 300 × g for 10 minutes to collect the cell pellets. All cell pellets were resuspended in 200 μL of DPBS, which was used for cell culture on the pico-porous nanostructured chips.

B. COMPUTER-AUDED TARGET CELLS IDENTIFICATION

In addition, the identification and counting of captured CTCs are important. CTCs identification relies on the interpretation of immunofluorescence images of the candidate cells. Traditional cell identification procedures are time consuming and difficult to standardize. The judgment of CTCs relies on various subjective criteria among analysts. Computer-aided identification research has recently started, but little progress has been made in this regard. The most common criterion for cell judgment depends on the size and shape of the cell image [41]. Some studies have incorporated machine learning techniques [42], such as convolutional neural networks (CNNs) [43] and transfer learning methods [44].

Instead of manual counting, computer-aided cell image processing was used to analyze the full image of the entire chip, which was captured using a fluorescence microscope. For the analysis, the cells were required to have both the cytoplasm stained with CellTracker™Green and the cell nucleus stained with DAPI. The staining intensity of cells with CellTracker™Green and DAPI was at least twice that of the background. The candidate cell region length and width must be greater than 3 μm for DAPI, and greater than 4 μm for the green area. The presence of CTCs was determined by identifying cells that exhibited passive staining with CellTracker™Green and DAPI to eliminate mis-staining of particles. When these conditions are satisfied, they can be considered as cells and their quantities can be calculated and evaluated. This computer-aided method reduced the overall analysis and identification time from 3 hours to less than 30 minutes. Fig. 5(a) shows the distribution of cells on the chip (the display area is approximately 2.28 mm × 1.4 mm). The first column of the cell images in Fig. 5(b) was stained with DAPI, the second column was stained with CellTracker™Green, and the third column shows the merged image. The cytokeratin size ranged from 22 μm. to 31 μm. Fig. 5(b) displays the individual details of the cells in Fig. 5(a). Fig. 5(c) shows the top view of the H1975 cells on the chip. Fig. 5(d) H1975 cells close-up photo. All the cells in Fig. 5 were intact, and no cell deformation was caused by shear stress. It had well demonstrated the functionality of nanostructured silicon surface for the capturing of CTCs.

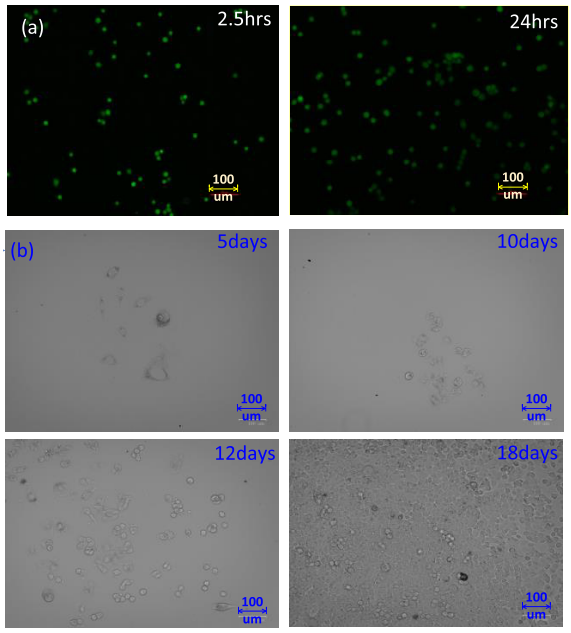

FIGURE 6. (a) Evaluation of stained H1975 cells viability on the nanostructured chip; (b) After 18 days of long-term cell culture, the culture flask was observed to be full of cells.

V. DESCRIPTIONS OF CELL CAPTURE AND CULTURE

A. CIRCULATING TUMOR CELLS CAPUTURE

The liquid specimen mixed with H1975 cells was injected into the microcavity biosensing with nanostructured chips, and 1082 cells were captured. When conducting the same experiment synchronously with non-nanostructured silicon chips in microcavity biosensing, only 104 cells were captured. This means that the nanostructured chips enhance the capture rate by a factor of 10, owing to their cell-friendly microenvironment.

In addition, the target cells captured by microcavity biosensing showed less than 5% cell damage in the cell image, which was lower than approximately 20% damage experienced when traditional microfluidic devices were used.

B. LIVE TARGET CELLS CULTURED AFTER CAPUTRE

In addition to a high cell capture rate, another crucial point is that the captured cells experience less damage and loss. If it can be effectively and successfully cultured, it can be used as a successful capture structure. To confirm the cultivation of living cancer cells on nanostructured chips, 22,000 living H1975 cells were placed on the chips. Then,

using the LIVE/DEAD®Viability/Cytotoxicity Kit (Thermo Fisher Scientific, Eugene, OR, USA), fluorescent staining (Calcein AM and Ethidium homodimer-1) was performed on cultured H1975 cells. Dead cells were washed with DPBS after fluorescent staining. A microscope (Nikon ECLIPSE NiE, Japan) was used to observe the fluorescent expression of cell survival. Fig. 6(a) shows the results observed at 2.5 hours and 24 hours by staining, confirming the successful culturing of the cells. Fig. 6(b) shows long-term cell culture. After 72 hours of culture, cells were cut from the chips using trypsin and transferred to 25T culture flasks for further cultivation. A ZOE Fluorescent Cell Imager (Bio-Rad, USA) was used to monitor the cell culture conditions. Fig. 6 (b) shows that the target cells were not only well cultivated for 5, 10, and 12 days but also demonstrated a long-term cell culture lasting up to 18 days. This proves that this method does not damage cells, allowing them to continue to be cultured. Consequently, pico-porous nanostructured chips are suitable for long-term cultivation of H1975 cells. Fig. 3 shows the structural depth and surface density of the pico-porous nanostructured chips used in this study.

VI. CONCLUSION

This study utilized computer-aided cell image recognition to minimize human misjudgment and to reduce the analysis time to less than 30 minutes. These results demonstrated that using a microcavity biosensing device is a simple and efficient method for cell capture and culture. Compared with traditional narrow microfluidics, this structure has a larger cross-section and contact area, providing the advantage of a lower shear stress force. Microcavity biosensing includes a pair of surface-modified pico-porous nanostructured chips. Cell damage rate was maintained at below 5%. In addition, low-speed rotational shaking reduces cell accumulation and enhances the capture rate without affecting the target cells. Different from the works demonstrating the modeling of the vascular transport barrier by microfabricated blood vessels, a study of nanostructured chips imitating the environment of real human blood vessels can facilitate the cell pseudopods to attach and allow for better cell growth. Therefore, microcavity biosensing can provide a capture rate approximately 10 times higher than that of non-nanostructured chips, which is advantageous for long-term cell cultures lasting up to 18 days or longer. This type of structure allows the cells to proliferate effectively. In future applications, it can not only facilitate general cell capture and identification but can also be utilized for drug development experiments.

ACKNOWLEDGMENT

The authors would like to express their appreciation for the assistance provided by CytoAurora Biotechnologies Inc. (Wei-Cheng Hsu for sample preparation, and Guang-Ci Ye for their help with the measurements). Yu-Hsiang Tang and Nien-Nan Chu of the Instrument Technology Research Center (ITRC), National Applied Research Laboratories, Hsinchu, Taiwan, for their assistance with SEM imaging, and the Taiwan Semiconductor Research Institute (TSRI) Hsinchu, Taiwan, for chip manufacturing equipment.

REFERENCES

[1] R. J. Cote and R. H. Datar, *Circulating Tumor Cell*, 1st ed. Cham, Switzerland: Springer, 2016.

[2] E. Lefrançais, "The Lung is a site of platelet biogenesis and a reservoir for Hematopoietic progenitors," *Nature*, vol. 544, pp. 105–109, Apr. 2017.

[3] M. L. Jones, J. Siddiqui, K. J. Pienta, and R. H. Getzenberg, "Circulating fibroblast-like cells in men with metastatic prostate cancer," *Prostate*, vol. 73, no. 2, pp. 176–181, Jan. 2013.

[4] P. Danise, M. Maconi, F. Barrella, A. Di Palma, D. Avino, A. Rovetti, M. Gioia, and G. Amendola, "Evaluation of nucleated red blood cells in the peripheral blood of hematological diseases," *Clin. Chem. Lab. Med. (CCLM)*, vol. 50, no. 2, pp. 357–360, Jan. 2012.

[5] S. Zheng, H. K. Lin, B. Lu, A. Williams, R. Datar, R. J. Cote, and Y.-C. Tai, "3D microfilter device for viable circulating tumor cell (CTC) enrichment from blood," *Biomed. Microdevices*, vol. 13, no. 1, pp. 203–213, Feb. 2011.

[6] M. Boya, T. Ozkaya-Ahmadov, B. E. Swain, C.-H. Chu, N. Asmare, O. Civelekoglu, R. Liu, D. Lee, S. Tobia, S. Biliya, L. D. McDonald, B. Nazha, O. Kucuk, M. G. Sanda, B. B. Benigno, C. S. Moreno, M. A. Bilen, J. F. McDonald, and A. F. Sarioglu, "High throughput, label-free isolation of circulating tumor cell clusters in meshed microwells," *Nature Commun.*, vol. 13, no. 1, p. 3385, Jun. 2022.

[7] D. F. Hayes, M. Cristofanilli, G. T. Budd, M. J. Ellis, A. Stopeck, M. C. Miller, J. Matera, W. J. Allard, G. V. Doyle, and L. W. W. M. Terstappen, "Circulating tumor cells at each follow-up time point during therapy of metastatic breast cancer patients predict progression-free and overall survival," *Clin. Cancer Res.*, vol. 12, no. 14, pp. 4218–4224, Jul. 2006.

[8] L. Wang, "Promise and limits of the CellSearch platform for evaluating pharmacodynamics in circulating tumor cells," *Seminars Oncol.*, vol. 43, no. 4, pp. 464–475, Aug. 2016.

[9] A. Garraud, C. Velez, Y. Shah, N. Garraud, B. Kozissnik, E. G. Yarmola, K. D. Allen, J. Dobson, and D. P. Arnold, "Investigation of the capture of magnetic particles from high-viscosity fluids using permanent magnets," *IEEE Trans. Biomed. Eng.*, vol. 63, no. 2, pp. 372–378, Feb. 2016.

[10] S. Nagrath, L. V. Sequist, S. Maheswaran, D. W. Bell, D. Irimia, L. Ulkus, M. R. Smith, E. L. Kwak, S. Digumarthy, A. Muzikansky, P. Ryan, U. J. Balis, R. G. Tompkins, D. A. Haber, and M. Toner, "Isolation of rare circulating tumour cells in cancer patients by microchip technology," *Nature*, vol. 450, no. 7173, pp. 1235–1239, Dec. 2007.

[11] F. Caselli, A. De Ninno, R. Reale, L. Businaro, and P. Bisegna, "A Bayesian approach for coincidence resolution in microfluidic impedance cytometry," *IEEE Trans. Biomed. Eng.*, vol. 68, no. 1, pp. 340–349, Jan. 2021.

[12] F. D. Schwab, M. C. Scheidmann, L. L. Ozimski, A. Kling, L. Armbrecht, T. Ryser, I. Krol, K. Strittmatter, B. D. Nguyen-Sträuli, F. Jacob, A. Fedier, V. Heinzelmann-Schwarz, A. Wicki, P. S. Dittrich, and N. Aceto, "MyCTC chip: Microfluidic-based drug screen with patient-derived tumour cells from liquid biopsies," *Microsystems Nanoeng.*, vol. 8, no. 1, p. 130, Dec. 2022.

[13] H. Shafiee, M. B. Sano, E. A. Henslee, J. L. Caldwell, and R. V. Davalos, "Selective isolation of live/dead cells using contactless dielectrophoresis (cDEP)," *Lab Chip*, vol. 10, no. 4, p. 438, 2010.

[14] V. Shirmohammadli and N. Manavizadeh, "Numerical modeling of cell trajectory inside a dielectrophoresis microdevice designed for breast cancer cell screening," *IEEE Sensors J.*, vol. 18, no. 20, pp. 8215–8222, Oct. 2018.

[15] J. Guo, W. Lei, X. Ma, P. Xue, Y. Chen, and Y. Kang, "Design of a fluidic circuit-based microcytometer for circulating tumor cell detection and enumeration," *IEEE Trans. Biomed. Circuits Syst.*, vol. 8, no. 1, pp. 35–41, Feb. 2014.

[16] Y. Ning, C. Multari, X. Luo, C. Palego, X. Cheng, J. C. M. Hwang, A. Denzi, C. Merla, F. Apollonio, and M. Liberti, "Broadband electrical detection of individual biological cells," *IEEE Trans. Microw. Theory Techn.*, vol. 62, no. 9, pp. 1905–1911, Sep. 2014.

[17] M. Farina, F. Piacenza, F. De Angelis, D. Mencarelli, A. Morini, G. Venanzoni, T. Pietrangelo, M. Malavolta, A. Basso, M. Provinciali, J. C. M. Hwang, X. Jin, and A. Di Donato, "Investigation of fullerene exposure of breast cancer cells by time-gated scanning microwave microscopy," *IEEE Trans. Microw. Theory Techn.*, vol. 64, no. 12, pp. 4823–4831, Dec. 2016.

[18] C.-L. Chang, S. I. Jalal, W. Huang, A. Mahmood, D. E. Matei, and C. A. Savran, "High-throughput immunomagnetic cell detection using a microaperture chip system," *IEEE Sensors J.*, vol. 14, no. 9, pp. 3008–3013, Sep. 2014.
[19] J. Chung, D. Issadore, A. Ullal, K. Lee, R. Weissleder, and H. Lee, "Rare cell isolation and profiling on a hybrid magnetic/size-sorting chip," *Biomicrofluidics*, vol. 7, no. 5, Sep. 2013, Art. no. 054107.
[20] G. Nabovati, E. Ghafar-Zadeh, A. Letourneau, and M. Sawan, "Smart cell culture monitoring and drug test platform using CMOS capacitive sensor array," *IEEE Trans. Biomed. Eng.*, vol. 66, no. 4, pp. 1094–1104, Apr. 2019.
[21] H. Zhang, X. Lin, Y. Huang, M. Wang, C. Cen, S. Tang, M. R. Dique, L. Cai, M. A. Luis, J. Smollar, Y. Wan, and F. Cai, "Detection methods and clinical applications of circulating tumor cells in breast cancer," *Frontiers Oncol.*, vol. 11, Jun. 2021, Art. no. 652253.
[22] A. Tiwari, G. Punshon, A. Kidane, G. Hamilton, and A. M. Seifalian, "Magnetic beads (dynabead) toxicity to endothelial cells at high bead concentration: Implication for tissue engineering of vascular prosthesis," *Cell Biol. Toxicol.*, vol. 19, no. 5, pp. 265–272, Oct. 2003.
[23] S. Regmi, A. Fu, and K. Q. Luo, "High shear stresses under exercise condition destroy circulating tumor cells in a microfluidic system," *Sci. Rep.*, vol. 7, no. 1, p. 39975, Jan. 2017.
[24] Z. Sheidaei, P. Akbarzadeh, and N. Kashaninejad, "Advances in numerical approaches for microfluidic cell analysis platforms," *J. Sci., Adv. Mater. Devices*, vol. 5, no. 3, pp. 295–307, Sep. 2020.
[25] S. L. Stott, "Isolation of circulating tumor cells using a microvortex-generating herringbone-chip," *Proc. Nat. Acad. Sci. USA*, vol. 107, no. 43, pp. 18392–18397, Oct. 2010.
[26] M. Deliorman, F. K. Janahi, P. Sukumar, A. Glia, R. Alnemari, S. Fadl, W. Chen, and M. A. Qasaimeh, "AFM-compatible microfluidic platform for affinity-based capture and nanomechanical characterization of circulating tumor cells," *Microsyst. Nanoeng.*, vol. 6, no. 1, p. 20, Mar. 2020.
[27] Q. Shen, H. Yang, C. Peng, H. Zhu, J. Mei, S. Huang, B. Chen, J. Liu, W. Wu, and S. Cao, "Capture and biological release of circulating tumor cells in pancreatic cancer based on peptide-functionalized silicon nanowire substrate," *Int. J. Nanomedicine*, vol. 14, pp. 205–214, Dec. 2018.
[28] T. H. Kim, Y. Wang, C. R. Oliver, D. H. Thamm, L. Cooling, C. Paoletti, K. J. Smith, S. Nagrath, and D. F. Hayes, "A temporary indwelling intravascular aphaeretic system for in vivo enrichment of circulating tumor cells," *Nature Commun.*, vol. 10, no. 1, p. 1478, Apr. 2019.
[29] L. B. Leverett, J. D. Hellums, C. P. Alfrey, and E. C. Lynch, "Red blood cell damage by shear stress," *Biophysical J.*, vol. 12, no. 3, pp. 257–273, Mar. 1972.
[30] S.-C. Lien, S.-F. Chang, P.-L. Lee, S.-Y. Wei, M. D.-T. Chang, J.-Y. Chang, and J.-J. Chiu, "Mechanical regulation of cancer cell apoptosis and autophagy: Roles of bone morphogenetic protein receptor, Smad1/5, and p38 MAPK," *Biochimica et Biophysica Acta (BBA) Mol. Cell Res.*, vol. 1833, no. 12, pp. 3124–3133, Dec. 2013.
[31] F. J. Armistead, J. G. De Pablo, H. Gadêlha, S. A. Peyman, and S. D. Evans, "Cells under stress: An inertial-shear microfluidic determination of cell behavior," *Biophys. J.*, vol. 116, no. 6, pp. 1127–1135, Mar. 2019.
[32] B. Wojciak-Stothard and A. J. Ridley, "Shear stress–induced endothelial cell polarization is mediated by rho and rac but not Cdc42 or PI 3-kinases," *J. Cell Biol.*, vol. 161, no. 2, pp. 429–439, Apr. 2003.
[33] W. Kim, J. K. Ng, M. E. Kunitake, B. R. Conklin, and P. Yang, "Interfacing silicon nanowires with mammalian cells," *J. Amer. Chem. Soc.*, vol. 129, no. 23, pp. 7228–7229, Jun. 2007.
[34] C. E. Brennen, *Internet Book on Fluid Mechanics*. Ontario, CA, USA: Dankat, 2016.
[35] V. D. Bhat, G. A. Truskey, and W. M. Reichert, "Fibronectin and avidin-biotin as a heterogeneous ligand system for enhanced endothelial cell adhesion," *J. Biomed. Mater. Res.*, vol. 41, no. 3, pp. 377–385, Sep. 1998.
[36] J. M. Barnes, J. T. Nauseef, and M. D. Henry, "Resistance to fluid shear stress is a conserved biophysical property of malignant cells," *PLoS ONE*, vol. 7, no. 12, Dec. 2012, Art. no. e50973.
[37] H. Moghadas, M. S. Saidi, N. Kashaninejad, and N.-T. Nguyen, "Challenge in particle delivery to cells in a microfluidic device," *Drug Del. Transl. Res.*, vol. 8, no. 3, pp. 830–842, Jun. 2018.
[38] I. Pereiro, A. Fomitcheva-Khartchenko, and G. V. Kaigala, "Shake it or shrink it: Mass transport and kinetics in surface bioassays using agitation and microfluidics," *Anal. Chem.*, vol. 92, no. 15, pp. 10187–10195, Aug. 2020.
[39] K. Ley, E. Lundgren, E. Berger, and K. Arfors, "Shear-dependent inhibition of granulocyte adhesion to cultured endothelium by dextran sulfate," *Blood*, vol. 73, no. 5, pp. 1324–1330, Apr. 1989.
[40] L. W. Kraiss, A. S. Weyrich, N. M. Alto, D. A. Dixon, T. M. Ennis, V. Modur, T. M. McIntyre, S. M. Prescott, and G. A. Zimmerman, "Fluid flow activates a regulator of translation, p70/p85 s6 kinase, in human endothelial cells," *Amer. J. Physiol.-Heart Circulatory Physiol.*, vol. 278, no. 5, pp. H1537–H1544, May 2000.
[41] M. Zhou, H. Zheng, Z. Wang, R. Li, X. Liu, W. Zhang, Z. Wang, H. Li, Z. Wei, and Z. Hu, "Precisely enumerating circulating tumor cells utilizing a multi-functional microfluidic chip and unique image interpretation algorithm," *Theranostics*, vol. 7, no. 19, pp. 4710–4721, 2017.
[42] X.-H. Han, J. Wang, G. Xu, and Y.-W. Chen, "High-order statistics of microtexton for HEp-2 staining pattern classification," *IEEE Trans. Biomed. Eng.*, vol. 61, no. 8, pp. 2223–2234, Aug. 2014.
[43] S. Wang, Y. Zhou, X. Qin, S. Nair, X. Huang, and Y. Liu, "Label-free detection of rare circulating tumor cells by image analysis and machine learning," *Sci. Rep.*, vol. 10, no. 1, p. 12226, Jul. 2020.
[44] Z. Guo, X. Lin, Y. Hui, J. Wang, Q. Zhang, and F. Kong, "Circulating tumor cell identification based on deep learning," *Frontiers Oncol.*, vol. 12, Feb. 2022, Art. no. 843879.

SHENG-WEN CHEN received the B.S. and M.S. degrees in electronic engineering from Chung Yuan Christian University, Taiwan, in 1999 and 2003, respectively. He is currently pursuing the Ph.D. degree in electrical engineering with the National Chung Cheng University, Taiwan. His research interests include microfluidic-based devices, biosensor, semiconductor process, and RF circuit design.

JANNE-WHA WU (Member, IEEE) received the B.S.E.E. and master's degrees from the National Cheng Kung University, Taiwan, in 1988 and 1990, respectively, and the Ph.D. degree in electronics engineering from the National Chiao Tung University, Taiwan, in 1995. He worked on the RF power device characterization and RF power amplifier module at Hexawave, Inc., from 1997 to 1999. He joined Advanced Wireless Semiconductor Company in charge of GaAs HBT modeling and reliability analysis from 1999 to 2001. Subsequently, he was responsible for the development and production of mobile power amplifier in the component business group of Delta Electronics, Inc. from 2001 to 2005. He is currently an Associate Professor with the Department of Electrical Engineering and the Department of Communications Engineering, National Chung Cheng University, Taiwan.

CHUNG-ER HUANG received the B.S. degree in physics from Tamkang University, Taiwan, in 1993, and the Ph.D. degree in electronics engineering from the National Chiao Tung University, Taiwan, in 2002. He worked on the III-V HBT in Win Semiconductors Corporation from 2000 to 2004. He joined AzureWave Technologies, Inc. in charge of Wireless and System in Package (SiP) product from 2005 to 2015. He is currently a CEO of CytoAurora Biotechnologies, Inc., Taiwan.